Stable layer-building strategy to enhance cold-spray-based additive manufacturing

Hongjian Wu, Xinliang Xie, Meimei Liu, Christophe Verdy, Yicha Zhang, Hanlin Liao, Sihao Deng

Stable Layer-Building Strategy to Enhance Cold-Spray-Based Additive Manufacturing

Hongjian WU [a,1], Xinliang XIE [a,1], Meimei LIU [a], Christophe Verdy [a], Yicha ZHANG [b], Hanlin LIAO [a], Sihao DENG [a*]

a. ICB-PMDM-LERMPS UMR 6303, CNRS, UTBM, Université de Bourgogne Franche-Comté, 90010 Belfort, France

b. ICB-COMM UMR 6303, CNRS, UTBM, Université de Bourgogne Franche-Comté, 90010 Belfort, France

* Corresponding author: sihao.deng@utbm.fr (Sihao DENG)

[1] These authors have equal contributions to this work.

Abstract: Cold spray (CS) has recently become one of the popular additive manufacturing (AM) processes for its advantages: high-forming efficiency, low temperature, and no phase changing of materials. These advantages may make CS able to form large volume objects and possibly directly iterate with material-removing processes to become a hybrid AM process. Current research proposes using a bulk-based volume-forming strategy (e.g. a tessellation-based method) for volume building. Although it can form 3D volumes, the control of the process is difficult and it has limitations in forming complex 3D near-net-shapes with acceptable accuracy. This also conflicts with the basic principle of AM, where the volume forming is via the manner of layer by layer. To solve this problem for easy process control, this paper proposes a new spray strategy, one that considers the characteristics of cold spray and kinematic parameters, to enhance stable layer building for 3D shape forming. Both simulation and experiments are conducted for method verification. The benchmarking test on some basic objects shows better shape accuracy than existing methods, and the proposed process is easier to control, repeat and follow. This implies that the proposed method makes CS a real and ready layer-by-layer AM process for 3D shape forming.

Keywords: Cold spray; Additive manufacturing; Building strategy; Shape control; Coating model

1. Introduction

Additive manufacturing technology (also called rapid manufacturing or 3D printing) has been declared the first manufacturing 'revolution' of the 21st century by leading industry authorities. People now are exploring and developing different AM technologies to fabricate freestanding metal components for aviation, space, automotive, biomedical, and other industries. Nowadays, there are several types of AM technology that are being employed commercially, like selective laser melting (SLM) and selective laser sintering (SLS), as well as wire and arc additive manufacturing (WAAM) [1–5]. However, among these techniques, high-power electron beams or high-frequency laser radiations are used for heating or melting materials, which can lead to unsatisfactory results such as oxidations, grain growth, residual thermal stresses, and phase transformations.

Cold spray (CS) is a newly developed surface-coating technique discovered in the 1980s. In practice, sprayed powders are accelerated to critical velocity (500 to 1500 m/s) by high-pressure gas, undergoing plastic deformation and bonding together with a substrate [6]. Nowadays, materials such as metals, ceramics, polymers, composite materials, and nanocrystalline powders are successfully deposited by CS [7–11]. Moreover, many advantages make CS a potentially competitive technology. For example, being a non-thermal or low-temperature process, CS allows spraying thermally sensitive materials without the risk of melting, oxidation, thermal decomposition, crystallization, grain growth, or phase transformations; the high speed and energy of sprayed particles make CS have high deposition efficiency; the sprayed coating has excellence performance including structural homogeneity, high density, high purity, notable cohesive strength, and frequently moderate compressive residual stresses [12–15]. Therefore, CS has been applied to restore damaged metal components as a repairing technique as well as to fabricate freestanding metal components as an AM technology [16–25]. To date, some companies or research institutions have intensively invested in the cold spray additive manufacturing (CSAM) process and have achieved various results. For example, General Electric company (GE) builds large amounts of components for aviation's jet engines by using the CSAM system. They also used two robots to produce large metal components for the first time, where one robot held the component and moved it to a precise position, while the other one held the spray gun to spray materials on the component [23]. Titomic company has adopted the CS process to spray titanium or titanium alloy materials onto a scaffold to produce a load-bearing structure [24]. There is no doubt that CSAM will be more widely used in the field of direct metal manufacturing and will eventually develop and innovate in the direction of commercialisation.

However, it also has been noted that CSAM has some disadvantages, such as low spatial resolution and dimensional accuracy. Besides, the distribution and velocity of particles in the feedstock jet are uneven [26], which causes the distribution of particles to nearly approximate Gaussian distribution [27,28]. In practice, an axisymmetric de-Laval nozzle is often used to emerge high-speed particles. When the nozzle traverse speed is low or the number of scanning passes is more, a triangular coating profile will be formed and the subsequent deposition of particles will be difficult [16,26]. As the schematic of CS particle deposition, shown in Fig. 1, continuous spraying makes the single-track profile gradually change from a thin coating with high deposition efficiency at the beginning (as shown in Fig. 1a) to a triangular-like coating with low deposition efficiency (as shown in Fig. 1b). During the spray process, the velocity of particles in the centre of the feedstock jet is generally higher than that of those in the other areas. Furthermore, the absolute number and the size of particles deposited on the centre area of the track are larger than the particles on the edges. As a result, the thickness in the middle will increase significantly, making the impact angle of the particles near the centre line gradually decrease. It is well known that particles in the cold spray process need to reach a critical speed in order to produce plastic deformation to form a coating. Therefore, cold spraying is a process that is sensitive to the spray angle; an impact angle of 90° can achieve maximum deposition efficiency [29,30]. For particles with smaller spray angle, the velocity component perpendicular to the impact surface will not reach critical velocity, so it will rebound and dissipate without forming a coating. Therefore, the coating morphology slowly rising in the middle is not conducive to subsequent particle deposition. The impact angle decreases rapidly and the deposition rate decreases sharply, especially for the particles around the centre line [31]. Gradually, only particles in the centre can continue to deposit by the high-pressure gas. All this further exacerbates the difficulty of subsequent particle deposition, and eventually the area where particles can be deposited in the middle also continues to shrink to the point where it forms a triangular single-track profile [16,26]. Obviously, this characteristic would limit the application of CSAM for shape forming if the appropriate spraying method is not used. Although the idea of additive manufacturing by cold spraying has been proposed for a long time, there is no effective application for creating volumetric components in this field. Therefore, it is necessary to study the building strategy of CSAM to overcome its inherent limitations.

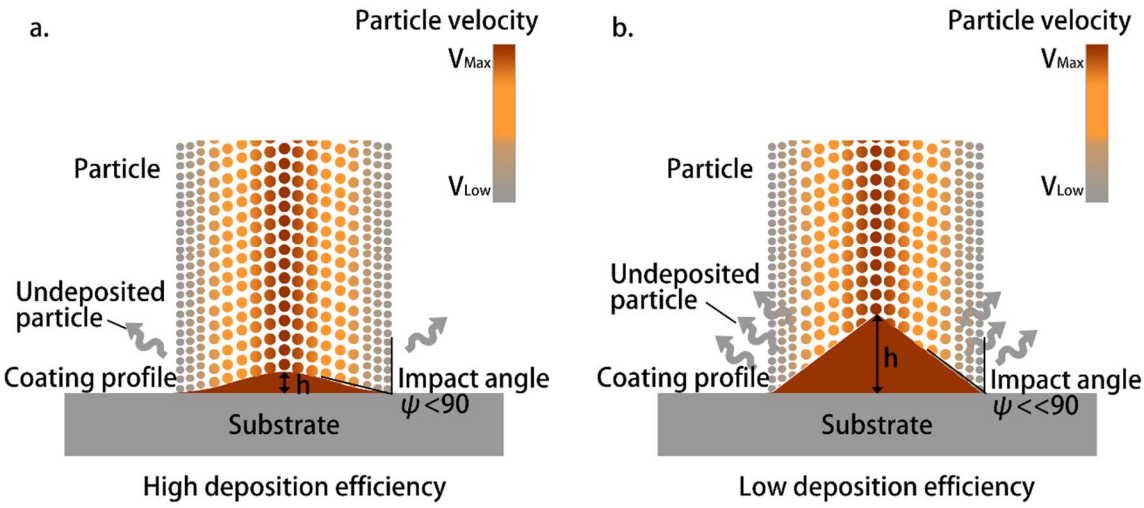

Fig. 1. Schematic of particle impact conditions in cases with (a) high deposition efficiency phase and (b) low deposition efficiency phase

In process benchmarking, local deposition of thick and vertical walls is always required to show the capability of forming complex components with diverse geometries. In order to build a thick and vertical wall without edge milling, J. Pattison et al. [16] proposed a strategy of triangular-tessellation. The process is to tilt the nozzle by a 4/5-axis system so that the current coating is sprayed perpendicularly onto the inclined surface of the previous track. However, they did not give any details on when the nozzle should be tilted and by which angle. Moreover, by using this method, a typical triangular-like shape should be generated before tilting the nozzle, as shown in Fig. 2. The particle impact conditions are not optimal in this case. Firstly, the typical triangular-like morphology influences overall deposition efficiency [26]. Such conditions can be attributed to the impact angle decrease, as mentioned above. It has been proved that the optimal impact angle in cold spray is 90° [28,32–34]. If the impact angle decreases, the deposition efficiency drops sharply. Secondly, high and sharp profiles can cause a tangential component of particle impact velocity, which may generate tensile forces and reduce total contact areas and bonding strength between the particles and the previously sprayed coating or substrate [33]. The porosity would also become greater [29,34]. Considering all the above-mentioned problems, this triangular-tessellation technique may not be a good solution for shape forming to obtain high-quality objects.

To solve the problems of CS for shape forming as discussed above, this study proposes a novel spray strategy that enables us to elaborate freeform 3D objects with acceptable precision. In view of the characteristic of CS deposition, three parameters are proposed to adjust the coating morphology in order to avoid forming triangular-like deposits. They are deflection angles θ, offsets s, and retreat distance d respectively, which will be

discussed in detail in the next section. Different combinations of these parameters were studied by a previously developed CS simulation model [30], which found that the setting of the three key parameters played a key role in determining the layer geometry, and thus the component built-up process. To compare with existing spray-coating strategies for additive forming, this paper also adopts the widely used benchmarking test shape, thick and vertical walls, to demonstrate the performance of the proposed new spray strategy. When additively building the walls or other thick coatings, the effective coating area can be fully covered without edge loss.

The remainder of this paper is organised as follows: Section 2 details the proposed strategy; Section 3 presents the numerical simulation and physical experiment procedure as well as illustrative results of benchmarking test and discussions; Section 4 draws a conclusion for this study and gives perspectives on future work.

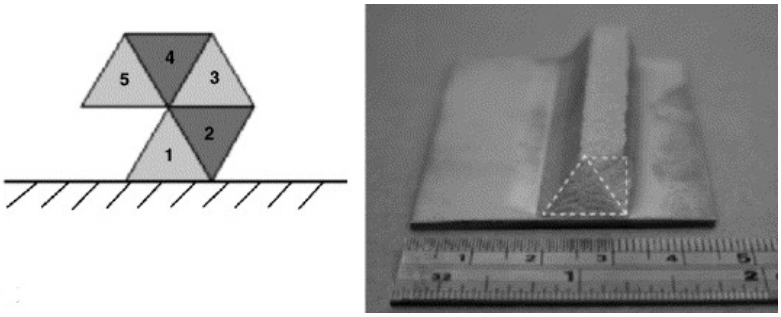

Fig. 2. Schematic of the triangular-tessellation strategy proposed by J. Pattison [16]

2. Spray strategies for CSAM

Starting with the deposition of simple coatings and ending with the fabrication of more complex components, it is always necessary to deposit thick and vertical walls, which is considered elementary geometry. In the CS process, the axisymmetric de-Laval nozzle can increase the velocity of gas and particles, thus it is widely used to form various coatings. Moreover, the growth of the coating is affected by the spray parameters such as gas pressure, temperature, and feedstock rate, as well as kinematic parameters including the nozzle scanning speed, the spray angle and the spray distance. Therefore, it is necessary to investigate the influence of different parameters on the shape and the height of the single track deposited by CS. Based on these results, a special spray strategy could be proposed for creating thick and vertical walls.

2.1. Experimental setup

In this study, a homemade CSAM system is applied to conduct the experiments. As shown in Fig. 3, the apparatus consists of a high-pressure compressed gas source, power sources, a powder feeder, a spray gun, and

an industrial robot (ABB IRB 2400). A computer in communication with the robot controller is used to program and simulate the experimental processes. An axisymmetric de-Laval nozzle with an expansion ratio of 8.3 was used in the experiments. The dimension details are displayed in Fig. 4.

Firstly, in order to reveal the relationship between operating parameters and as-sprayed coatings, and to help establish the specific numerical model of the coating profile to be used in section 3, single-track spraying experiments were carried out in this study. Due to the long response time of controlling spray parameters such as gas temperature, powder feed rate, etc., the experiments focused only on kinematic parameters which can be rapidly changed and controlled by the robot. Therefore, the variable parameters depended on different numbers of scanning pass, different nozzle traverse speeds, and different spray angles. A pure Cu powder with near-spherical morphology was used to deposit on Al substrates. The diameter range of powder is between 10 and 45 μm (average size of 26 μm). Fig. 5 shows the morphology and size distribution of the pure Cu powder. High-pressure air was applied as the propellant gas, and as powder carrier gas at a temperature of 500°C and a pressure of 3 MPa. The morphology of deposition was measured by a 3D profiler (LJ-V7060, Keyence, Japan). More detailed descriptions of the operating parameters are listed in Table.1.

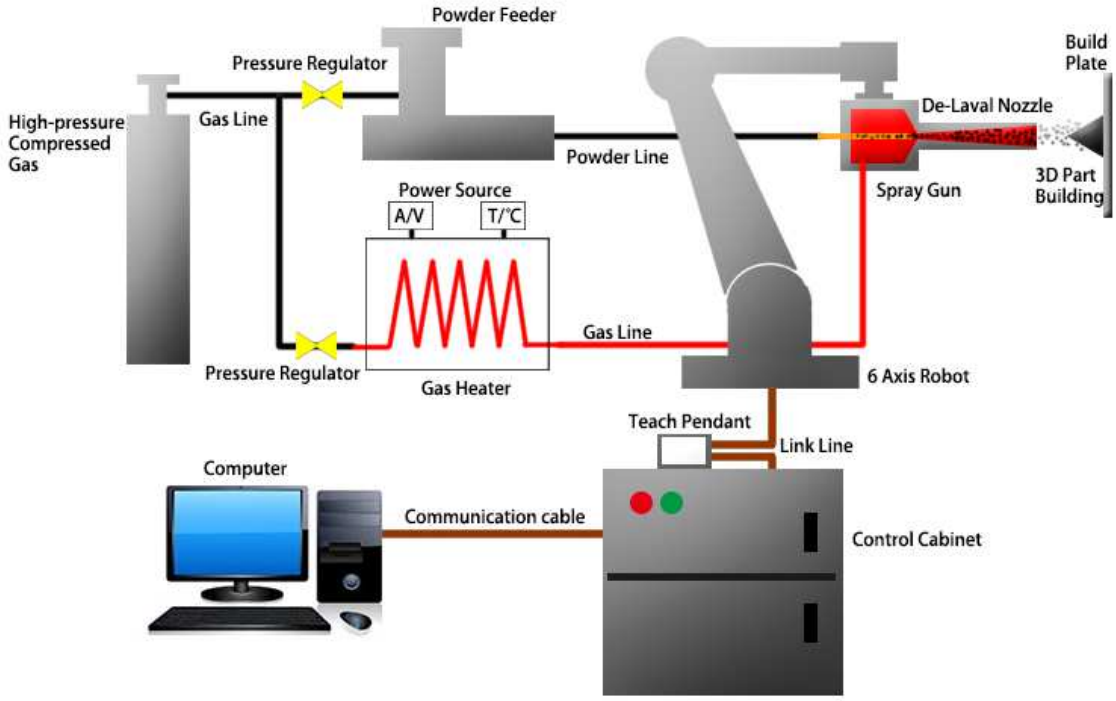

Fig. 3. Schematic diagram of the CSAM system

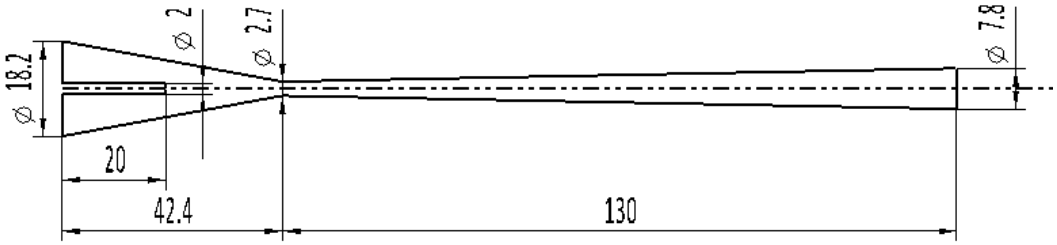

Fig. 4. Geometry diagram of axisymmetric de-Laval nozzle

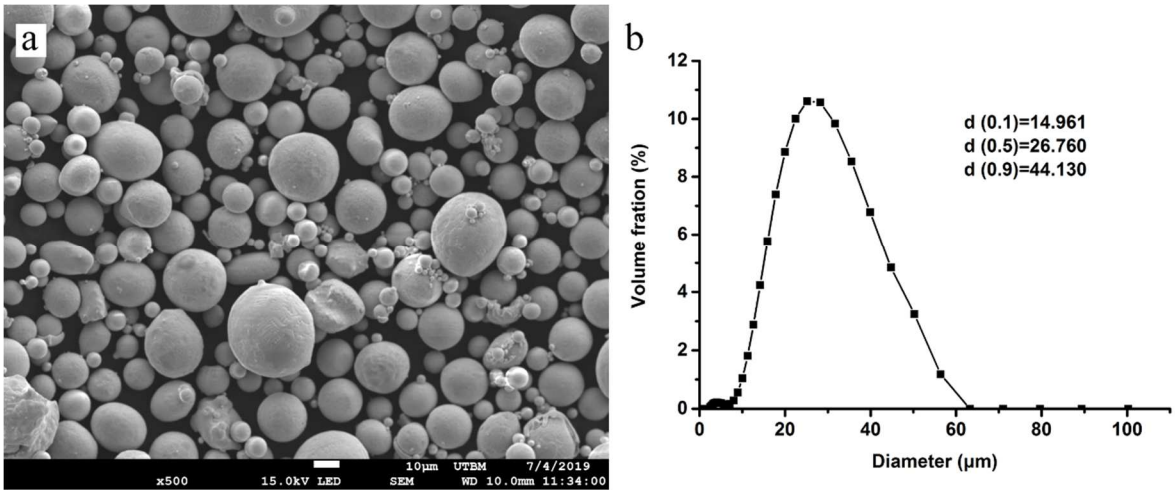

Fig. 5. SEM image of pure Cu powder used in experiments

Table. 1. Detailed description of operating parameters

Group	Nozzle traverse speed (mm/s)	Spray angle (°)	Powder feeding rate (g/min)	Spray distance (mm)	Number of scanning passes
1	100	90	24	30	1~20
2	20, 50, 100, 200	90	24	30	10
3	100	50, 60, 70, 80, 90	24	30	20

2.2. Single-track analysis

Fig. 6 shows the experiment results of group 1 in Table.1, which were carried out at different numbers of scanning passes while the other parameters were kept constant. It was found that the coating got thicker constantly and the shape of the single track became a triangle gradually when the number of scanning passes increased. Fig. 7 presents the experiment results of group 2 in Table.1. It shows that different nozzle traverse speeds can significantly change the height of the deposits, and a lower traverse speed will result in an increased coating thickness. Fig. 8 shows the results of group 3 in Table.1. It shows that the spray angles affect not only

deposition efficiency but also the shape of the track profile. The track asymmetry became more evident as the spray angle decreased.

The kinematic parameters are the main factors affecting the coating morphology in CS, and the deposits are bound to become triangular-like when the axisymmetric nozzle is used to spray continuously. If the kinematic parameters are not changed when spraying on the same regions, the particle impact condition will be worse. Therefore, it is important to avoid the tendency of triangular-like forming. An effective solution should be considered to ensure that the deposits can grow stably. Actually, if the height of deposits is low, then the impacting surface could be considered flat. Also, the impact surface can be kept flat by adjusting the kinematic parameters (such as spray angle) for every layer to avoid increasing the middle height of the coating, so that the deposits can grow up layer by layer.

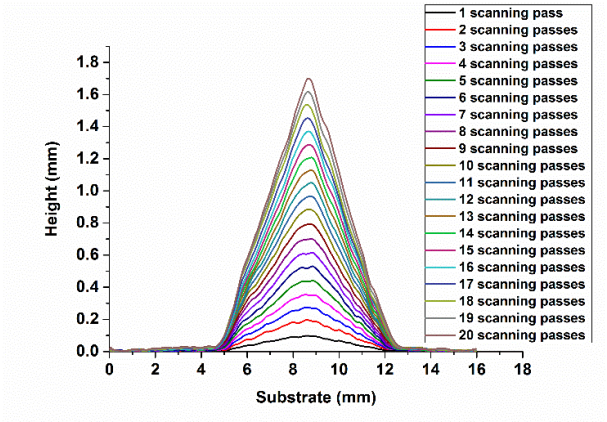

Fig. 6. Profiles of the single tracks deposited at different numbers of nozzle pass measured by the 3D profiler

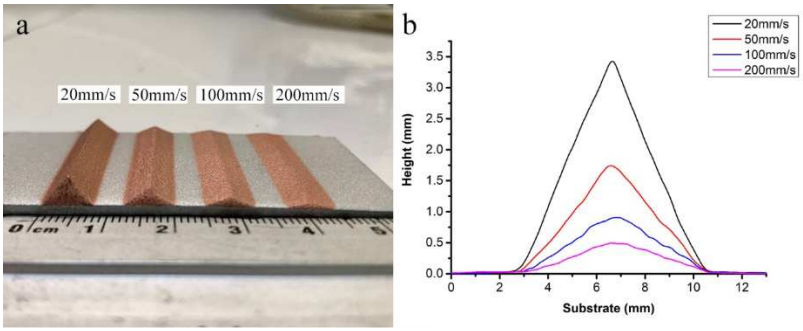

Fig. 7. (a) Single tracks deposited at different nozzle traverse speed (b) Profiles of single tracks measured by the 3D profiler

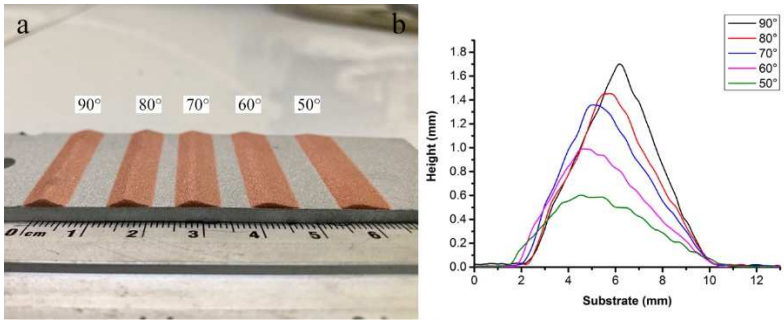

Fig. 8. (a) Single tracks deposited at different spray angles (b) Profiles of the single tracks measured by the 3D profiler

2.3. Spray strategy

According to the above analysis, a special spray strategy should be formulated to prevent CS deposits from developing into triangular shapes, which are usually associated with high porosity and low adhesion. Many researchers have suggested that the coating profile can be approximated as a symmetric Gaussian distribution curve [27,28]. A normal Gaussian curve is shown in Fig. 9; μ is the centre position of the peak and σ is the standard deviation. The values less than σ away from the mean account for 68.27% of the set, while the remaining portion is relatively low. Therefore, it is necessary to make mass distribution gradually concentrate on both sides. According to the above analysis, spray angles can change the symmetry, shifting the centre of gravity of the sprayed coatings in the direction of the incoming particles. Hence, the mass distribution of the layer can be uniformed by tilting the nozzle. Unlike the triangular-tessellation strategy, this spray strategy does not make triangular-like deposits before tilting the nozzle. The inclined spray manner is to compensate for the thickness difference between the middle and side of the deposit.

As displayed in Fig.10, three main parameters were proposed to control the shape of deposits: θ is the deflection angle in order to replenish particle depositions at the edge; s is the offset that can adjust the track width in horizon; d is the value that adjusts the retreat distance of the nozzle according to the growth height of layers. It can ensure that the spray distance between the top layer and the nozzle exit is consistent during spraying. Every layer is composed of a first track in the middle, a second track on the left, and a third one on the right. The first track should be controlled to avoid a triangular-like profile in the middle before performing the left and the right track. After spraying the left and the right track, the current layer could be formed as a flat surface before the next cycle. In this way, the single layer can steadily rise in a track-by-track manner without appearing to have defective triangular-like depositions. Meanwhile, this spray strategy also appropriates to fabricate large bricks or a thick coating (as shown in Fig. 11). The surface of the prescribed area is sprayed in a

perpendicular manner by specifying a scanning step of the corrected distribution. Then the edges are sprayed by tilting the nozzle to compensate for the edge loss.

Although the spraying strategy is mentioned above, how to choose the right value of parameters has become a key issue. It is indeed possible to conduct a large number of experiments through trial and error to explore the combination of parameters, but this will be very time-consuming and material-consuming. Through simulation, the coating morphology can be obtained in advance under the premise of using the current parameter set.

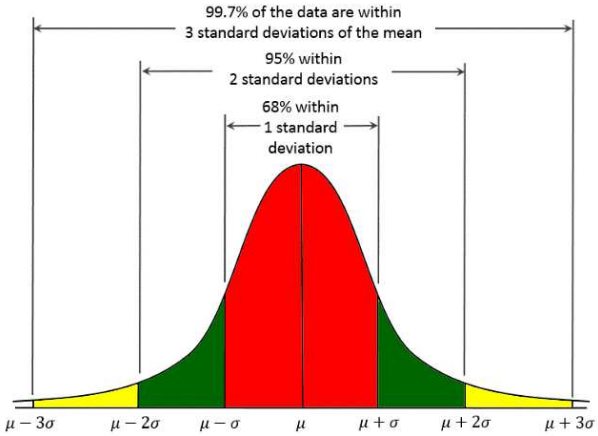

Fig. 9. Gaussian curve

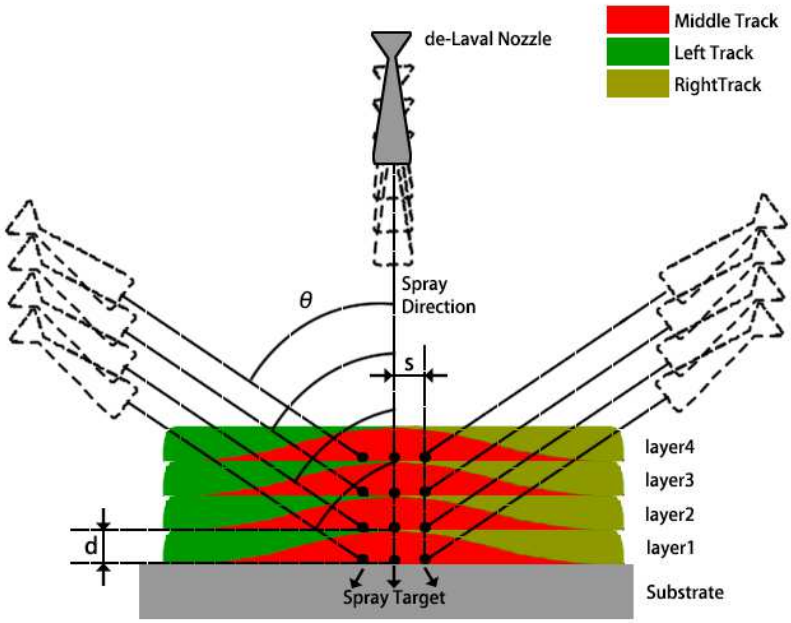

Fig. 10. Schematic of CSAM spray strategy for thick and vertical walls

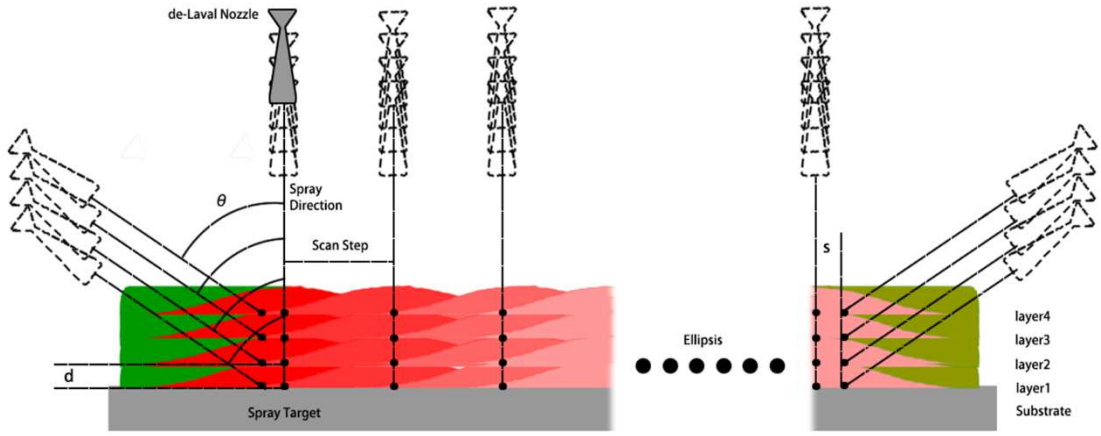

Fig. 11. Schematic of CSAM spray strategy for large blocks or thick coatings

3. Simulation and experimental verification

Simulation tests and validation experiments were carried out to verify the reliability of the proposed spray strategy. Here, the simulation can obtain instructive spraying parameters and prevent repeated spraying experiences. In addition, changes in deposits under current spray strategy can be observed more intuitively.

3.1. Simulation

In our previous work, a three-dimensional geometric model of the coating profile based on Gaussian distribution was developed for simulating coating thickness in CS [30]. A brief description of the simulation methodology is as follows. Firstly, the three-dimensional geometric model is represented by a Gaussian approximation function. This function takes into account the effect of spray parameters and kinematic parameters on deposition efficiency. Secondly, an algorithm couples the model with real robotic trajectories to simulate coating deposition in RobotStudio™ (ABB). Finally, the simulation results are presented in the graphical virtual environment.

Table.2 lists the detailed description of parameters used in the simulation. In the current simulation procedure, the first track is generated under normal parameters (in the case of perpendicular spray), as shown in Fig. 12a. It is a typical Gaussian profile. Then the left track, shown in Fig. 12b, is obtained by tilting angle of θ and offsetting distance of s to the left side. Thirdly, the right track is also created by the tilting angle of θ and the offsetting distance of s to the other side (see in Fig. 12c). The coating created by such operations can be considered one layer. Then the subsequent layers will be created on top of the previous layer following the same procedure. It was observed that the profile topography may change due to different parameters, and it was found

that the flatness and verticality of the formed profile are closely related to the combination of these parameters, while these two attributes are exactly the criteria for judging the quality of the control, reducing the post-machining to achieve net shape.

Table. 2. Detailed description of parameters used in simulation

Group	deflection angle θ (°)	offset distance s (mm)	nozzle retreat distance d (mm)
1	30	0, σ, 2σ, 3σ, 4σ	-
2	10, 20, 30, 40	2σ	-
3	30	2σ	0, Layer thickness

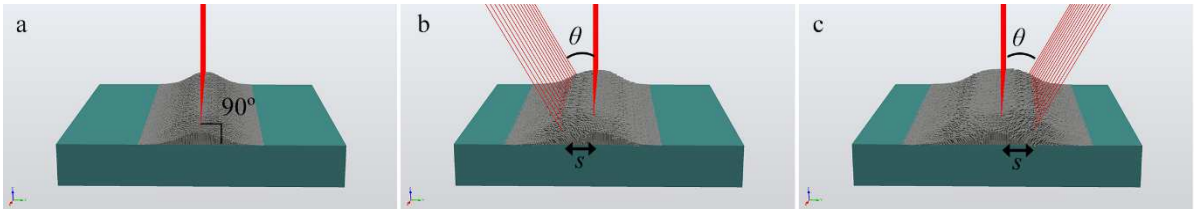

Fig. 12. Schematic of simulate operation

3.1.1 Simulation results and discussions

Fig.13 shows the results when the deflection angle is 30º (θ=30º) and only the offset distance s is changed (group 1 in Table.2). Fig.13 a1–a5 show the same situation after performing the first track, which is a typical Gaussian distribution coating profile in the case of vertical spray. Fig.13 b1–b5 show the second track superposed on the first one with different offset distance s of 0 mm, σ mm, 2σ mm, 3σ mm and 4σ mm, respectively. Fig.13 c1–c5 show the third track accumulated on the other side with the offset distance s of 0 mm, σ mm, 2σ mm, 3σ mm and 4σ mm, respectively. Fig.13 d1–d5 illustrate the deposit results in colour, which correspond to Fig.13 c1–c5, respectively, and their ranges are indicated by a colour bar. It can be found that the mass distribution gradually concentrated on both sides. But when the value of s is larger than three standard deviations, the peaks of mass appear again on both sides of the first track. According to the final results, it can be concluded that as s increases, the width of track increases, while the flatness increases initially and then decreases.

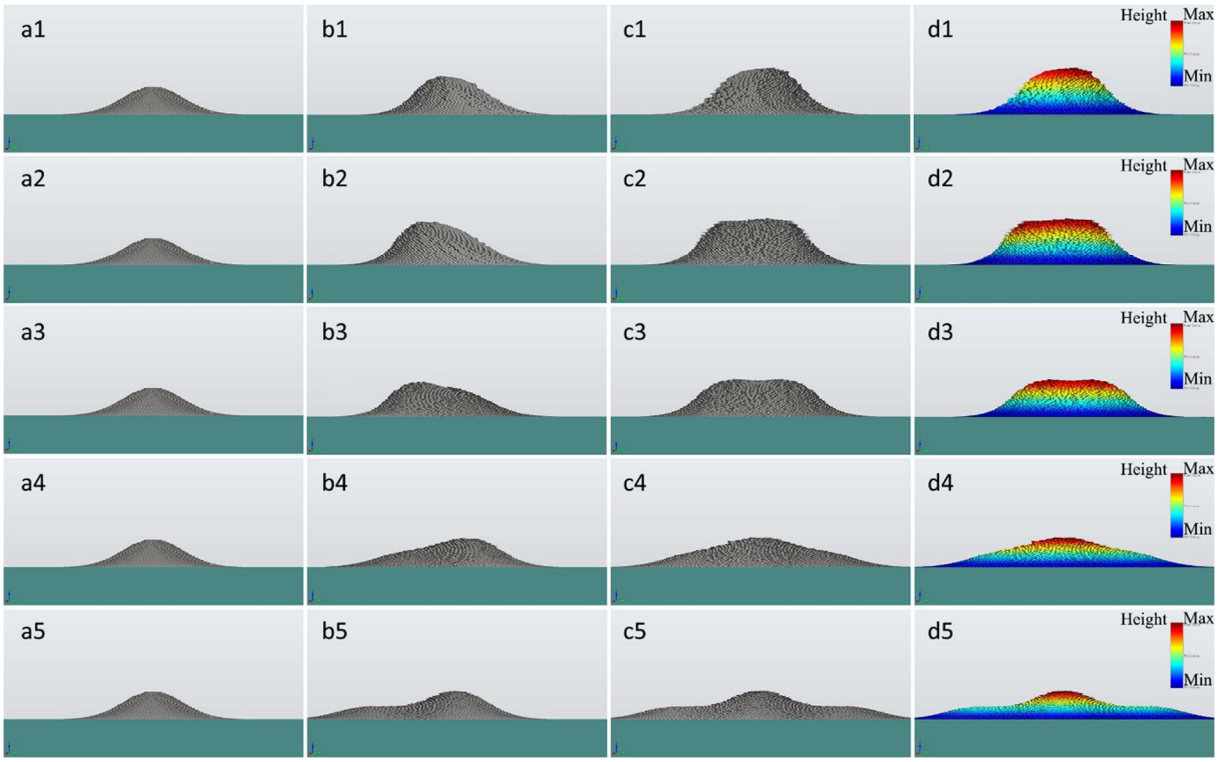

Fig. 13. Lateral view of spray strategy simulation in a situation where the deflection angle was 30º (θ=30º), and the offset distance s changed

Fig.14 shows the simulation results in a case where the offset distance s is fixed at 2σ and the deflection angle is changed (group 2 in Table.2). Fig.14 a1–a5 show the first track, which is a typical Gaussian distribution coating profile. Fig.14 b1–b4 show the second track when the deflection angle θ is 10º, 20º, 30º, and 40º, respectively. Fig.14 c1–c4 show the third track by the deflection angle θ of 10º, 20º, 30º, 40º, respectively. Fig.14 d1–d4 show the results represented in colour corresponding to Fig.14 c1–c4, respectively. It can be found that as θ increased, the mass distribution gradually concentrated on the side. However, increasing θ means reducing the spray angle, which will reduce deposition efficiency. When the deflection angle is 40º, the mass is concentrated in the middle and the flatness is decreased. According to the final results, it can be concluded that as θ increases, flatness initially increases and then decreases. However, θ cannot be too large because it will significantly reduce deposition efficiency.

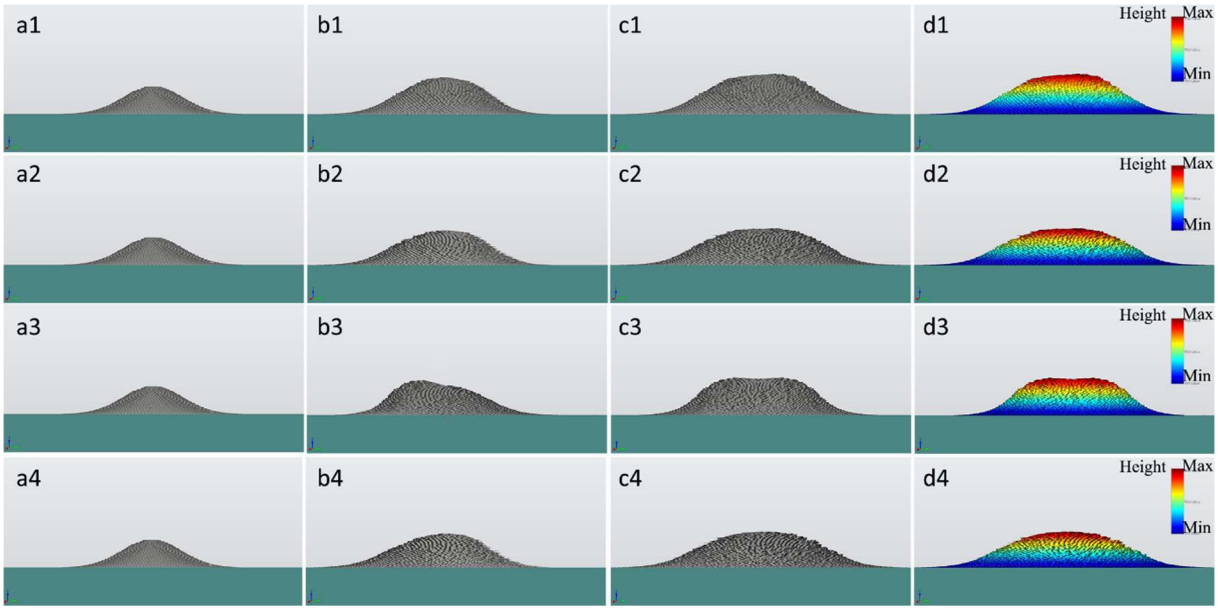

Fig. 14. Lateral view of spray strategy simulation in a situation where the offset distance was 2σ (s=2σ), and the deflection angle θ changed

Fig. 15 shows the comparison results between appending d (the value of nozzle retreat distance) and without it (group 3 in Table.2). The value of d equals the height of the layer. Fig.15 a1 and a2 show the first layer, which is formed at a deflection angle of 30 ° and an offset distance of 2σ mm. Fig.15 b1 and b2 show the first + second layers. However, the result in Fig.15 b2 was obtained by appending d, while Fig.15 b1 does not. It can be found that the flatness decreases without appending d while the other case can obtain the desired flatness. After spraying the third layer, the deposit in Fig. 15 d2 can keep flat while the deposits in Fig. 15 d1 become uneven. Therefore, the value of nozzle retreat can ensure the required flatness and the stable growth of the deposits.

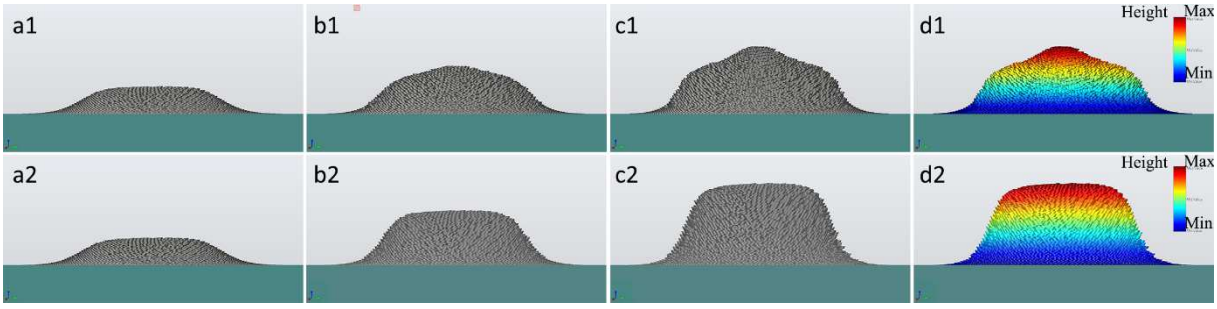

Fig. 15. Results comparison between without and with retreat distance d

Thus, the effects of three parameters have been studied in term of simulation, so that the experimental validation can be carried out to verify the reliability of the model, and to build the vertical wall and some basic volumetric components by using the optimal set of parameters.

3.2 Experiment

In the experiment, the apparatus and equipment, including the nozzle, are the same as used in the above single-track experiments. The pure Cu powder (the same powder as the above-mentioned section) with a feeding rate of 24 g/min was used to deposit on Al substrates. The temperature and the pressure of the compressed air were 500°C and 3 MPa, respectively. The nozzle traverse speed was defined as 100 mm/s. The spray distance was kept at 30 mm. The morphology of deposits was measured by the 3D profiler. Last but not least, due to the moving system being in charge of the industrial robot, the tool centre point (TCP) needed to be defined precisely to ensure the accuracy of the spray.

3.2.1. Experiment results and discussion

Fig. 16 shows the deposits profile curves measured by the 3D profiler, with a deflection angle of 30º (θ=30º), and the offset distance of 0 mm, σ mm, 2σ mm, 3σ mm, 4σ mm, respectively. They were indicated by lines of different colours. It was found that when s was 0 mm and σ mm, the deposits profile tended to become triangular-like; when s was 3σ mm, 4σ mm, the efficiency was dissatisfying; when s was 2σ mm, the deposits had a flat top surface and good efficiency. Fig. 17 shows the results with an offset distance of 2σ mm and the deflection angles of 10º, 20º, 30º, and 40º. Obviously, when θ was 40º, the efficiency was not good, while the deposits tended to form triangles with the deflection angles of 10º and 20º. Conclusively, these profiles proved that the value of deflection angle and offset distance can definitely affect the flatness and the efficiency of deposits, as discussed previously.

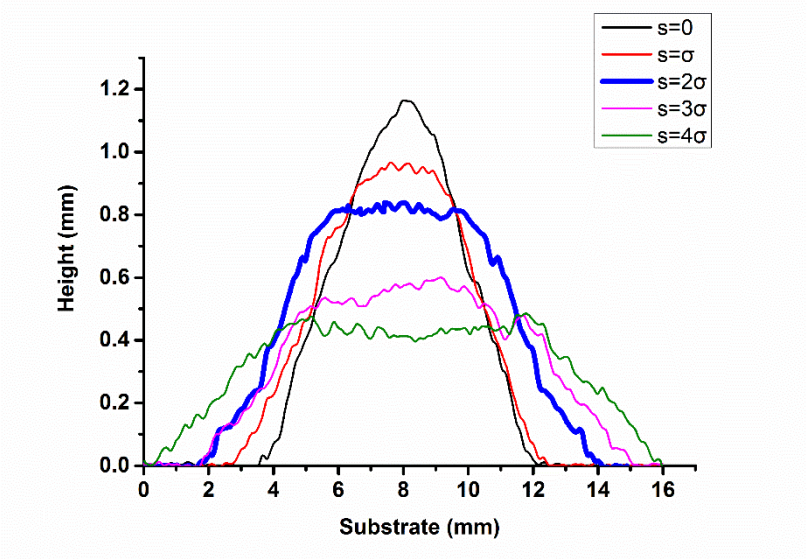

Fig. 16. Experiment results at the deflection angle of 30º (θ = 30º), and the offset distance was 0 mm, σ mm, 2 σ mm, 3 σ mm, 4 σ mm, respectively (s = was 0 mm, σ mm, 2 σ mm, 3 σ mm, 4 σ mm)

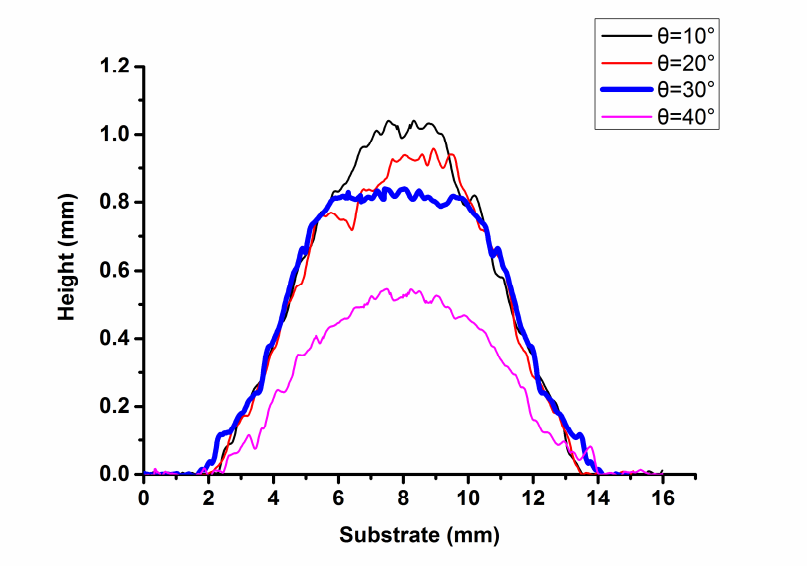

Fig. 17. Experiment results at the offset distance of 2 σ mm (s= 2 σ mm), and the deflection angle was 10º, 20º, 30º, 40º, respectively (θ =10º, 20º, 30º, 40º)

Fig. 18 illustrates the results of multiple layers. The value of nozzle retreat distance was set to 0.4 mm in order to make the deposits grow stably in the preconceived manner. Fig. 18a illustrates cross-section image of pure Copper-aluminum samples produced by the spray strategy with the axisymmetric de-Laval nozzle, taken by the optical microscope. It can be observed that the profile is not a typical CS triangular-like, and the upper surface has a substantially large and flat area, which created quite favourable conditions for the subsequent deposition of particles. Besides, the coating was dense and had no obvious cracks. The partial enlargement view showed the sample etched to reveal the particle/particle boundaries (as shown in Fig. 18a′). The particles appear to be tightly bonded. There were some pores in the coating, and the porosity was calculated to about 0.4% using imaging software (ImageJ). Fig. 18b shows the results of each sprayed track measured by the 3D profiler. Lines of different colours are used to distinguish the profile of different tracks. The growth of the coating in the processing can be observed. The deposits could basically be formed in the preconceived manner, as confirmed by the simulation in the previous section. It is obvious that layer-by-layer deposition permits the coating to grow stably without forming triangular morphology.

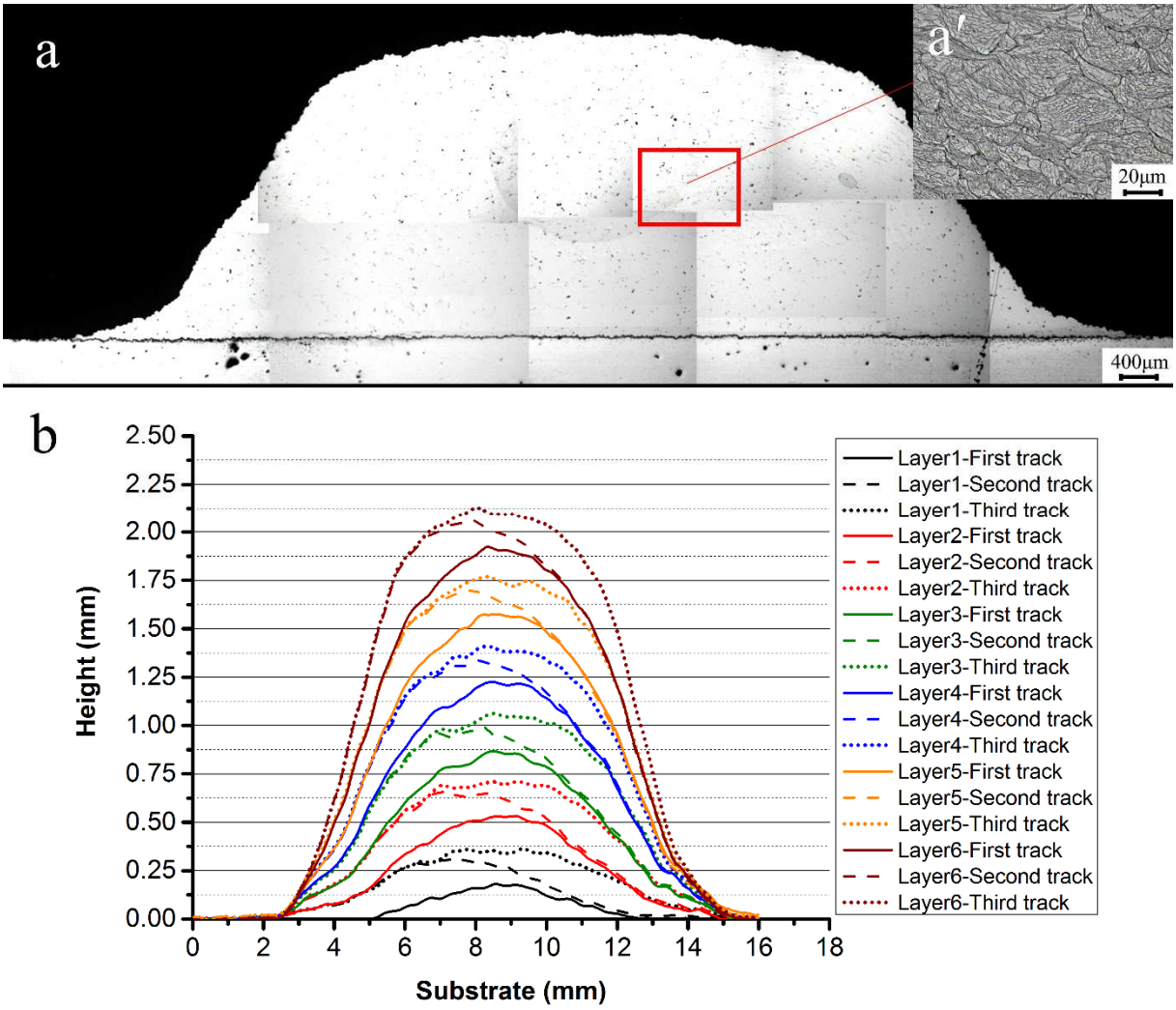

Fig. 18. (a) Cross-sectional view sprayed track using optical microscope; (a′) Optical micrograph of coatings (b) Each sprayed track morphology measured by a 3D profiler

Moreover, this spray strategy can be applied to build blocks or thick coatings on prescribed areas without edge losses. Fig. 19 shows thick coatings on the prescribed area. It can be seen that the normal spray strategy leads to edge losses. This means that during the coating formation, the area of the upper surface shrinks (more than 34% in this case). While the same coating was sprayed by performing this strategy, the borders were compensated without edge losses. The coating grew layer by layer, and the effective area reached nearly 100%. Finally, based on the presented spray strategy, different shaped samples were created successfully. As Fig. 20 illustrates, thick and vertical walls could be built on both a flat surface (Fig. 20a, b, and c) and on a curved surface (Fig. 20d). It proved that this method can be used for shape control and production of more complex components in cold spray additive manufacturing.

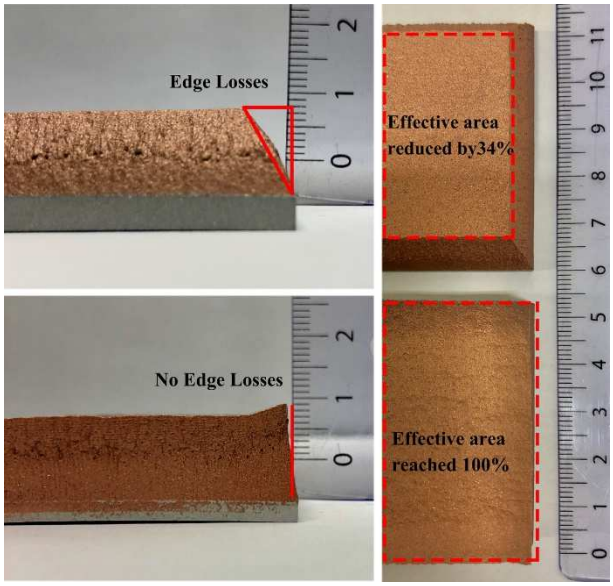

Fig. 19. Creation of thick coatings

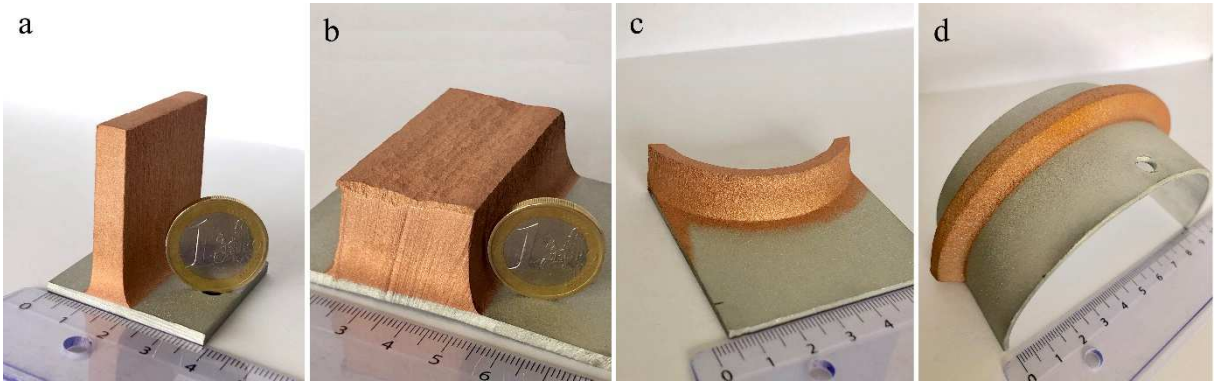

Fig. 20. (a) a thick and vertical wall was created on a flat surface; (b) a block was created on a flat surface; (c) a thick and vertical curved wall was created on a flat surface; (d) a thick and vertical wall was created on a curved surface.

4. Conclusion

Both industrial and academic communities are paying more and more attention to CS-based AM, especially for direct manufacturing of soft metal components. A stable layer-by-layer building strategy and capability of CS is a key preliminary step for forming complex 3D shapes in an additive way. This paper focused on the spraying parameters, considering the kinematic factors and the coating morphology characteristics of CS, in order to develop a stable layer-building strategy. Numerical simulation and actual benchmarking case study validate the proposed method, and the proper parameters that can establish the best stable layer in the current system are: the deflection angle θ is 30°, the offset distance s is 2σ mm and the nozzle retreat distance d is the layer thickness. It implies that more complex 3D geometries can be built by using this proposed layer-building strategy and

sophisticated coating scanning paths. Future work will further investigate the impact of nozzle shape and size on the layer building and the development of a multi-axis robotic tool-path planning strategy for building complex 3D curved layers or freeform 3D objects in near-net-shape with the proposed layer-building method.

Acknowledgments

The authors Hongjian WU, Xinliang XIE and Meimei LIU would like to acknowledge the support from the China Scholarship Council.

References

[1] X. Yan, S. Yin, C. Chen, C. Huang, R. Bolot, R. Lupoi, M. Kuang, W. Ma, C. Coddet, H. Liao, Effect of heat treatment on the phase transformation and mechanical properties of Ti6Al4V fabricated by selective laser melting, J. Alloys Compd. 764 (2018) 1056–1071. https://doi.org/10.1016/j.jallcom.2018.06.076

[2] J.-P. Kruth, P. Mercelis, J.V. Vaerenbergh, L. Froyen, M. Rombouts, Binding mechanisms in selective laser sintering and selective laser melting, Rapid Prototyp. J. (2005). https://doi:10.1108/13552540510573365.

[3] X. Yan, S. Yin, C. Chen, R. Jenkins, R. Lupoi, R. Bolot, W. Ma, M. Kuang, H. Liao, J. Lu, M. Liu, Fatigue strength improvement of selective laser melted Ti6Al4V using ultrasonic surface mechanical attrition, Mater. Res. Lett. 7 (2019) 327–333. https://doi:10.1080/21663831.2019.1609110.

[4] W.E. Frazier, Metal Additive Manufacturing: A Review, J. Mater. Eng. Perform. 23 (2014) 1917–1928. https://doi:10.1007/s11665-014-0958-z.

[5] X. Yan, R. Lupoi, H. Wu, W. Ma, M. Liu, G. O'Donnell, S. Yin, Effect of hot isostatic pressing (HIP) treatment on the compressive properties of Ti6Al4V lattice structure fabricated by selective laser melting, Mater. Lett. 255 (2019) 126537. https://doi.org/10.1016/j.matlet.2019.126537

[6] R.C. Dykhuizen, M.F. Smith, Gas dynamic principles of cold spray, J. Therm. Spray Technol. 7 (1998) 205–212. https://doi.org/10.1361/105996398770350945

[7] X. Xie, C. Chen, Y. Ma, Y. Xie, H. Wu, G. Ji, E. Aubry, Z. Ren, H. Liao, Influence of annealing treatment on microstructure and magnetic properties of cold sprayed Ni-coated FeSiAl soft magnetic composite coating, Surf. Coat. Technol. (2019). https://doi.org/10.1016/j.surfcoat.2019.05.008

[8] Q. Wang, K. Spencer, N. Birbilis, M.-X. Zhang, The influence of ceramic particles on bond strength of cold spray composite coatings on AZ91 alloy substrate, Surf. Coat. Technol. 205 (2010) 50–56. https://doi:10.1016/j.surfcoat.2010.06.008.

[9] P.C. King, A.J. Poole, S. Horne, R. de Nys, S. Gulizia, M.Z. Jahedi, Embedment of copper particles into polymers by cold spray, Surf. Coat. Technol. 216 (2013) 60–67. https://doi:10.1016/j.surfcoat.2012.11.023.

[10] L. Ajdelsztajn, J.M. Schoenung, B. Jodoin, G.E. Kim, Cold spray deposition of nanocrystalline aluminum alloys, Metall. Mater. Trans. A. 36 (2005) 657–666. https://doi:10.1007/s11661-005-0182-4.

[11] H.-K. Kang, S.B. Kang, Tungsten/copper composite deposits produced by a cold spray, Scr. Mater. 49 (2003) 1169–1174. https://doi:10.1016/j.scriptamat.2003.08.023.

[12] T. Suhonen, T. Varis, S. Dosta, M. Torrell, J.M. Guilemany, Residual stress development in cold sprayed Al, Cu and Ti coatings, Acta Mater. 61 (2013) 6329–6337. https://doi:10.1016/j.actamat.2013.06.033.
[13] C.J. Huang, X.C. Yan, W.Y. Li, W.B. Wang, C. Verdy, M.P. Planche, H.L. Liao, G. Montavon, Post-spray modification of cold-sprayed Ni-Ti coatings by high-temperature vacuum annealing and friction stir processing, Appl. Surf. Sci. 451 (2018) 56–66. https://doi:10.1016/j.apsusc.2018.04.257.
[14] C. Chen, Y. Xie, X. Yan, S. Yin, H. Fukanuma, R. Huang, R. Zhao, J. Wang, Z. Ren, M. Liu, Effect of hot isostatic pressing (HIP) on microstructure and mechanical properties of Ti6Al4V alloy fabricated by cold spray additive manufacturing, Addit. Manuf. 27 (2019) 595–605. https://doi.org/10.1016/j.addma.2019.03.028
[15] H. Assadi, F. Gärtner, T. Stoltenhoff, H. Kreye, Bonding mechanism in cold gas spraying, Acta Mater. 51 (2003) 4379–4394. https://doi.org/10.1016/S1359-6454(03)00274-X
[16] J. Pattison, S. Celotto, R. Morgan, M. Bray, W. O'neill, Cold gas dynamic manufacturing: A non-thermal approach to freeform fabrication, Int. J. Mach. Tools Manuf. 47 (2007) 627–634. https://doi.org/10.1016/j.ijmachtools.2006.05.001
[17] A. Sova, S. Grigoriev, A. Okunkova, I. Smurov, Potential of cold gas dynamic spray as additive manufacturing technology, Int. J. Adv. Manuf. Technol. 69 (2013) 2269–2278. https://doi.org/10.1007/s00170-013-5166-8
[18] R.N. Raoelison, C. Verdy, H. Liao, Cold gas dynamic spray additive manufacturing today: Deposit possibilities, technological solutions and viable applications, Mater. Des. 133 (2017) 266–287. https://doi.org/10.1016/j.matdes.2017.07.067
[19] S. Yin, P. Cavaliere, B. Aldwell, R. Jenkins, H. Liao, W. Li, R. Lupoi, Cold spray additive manufacturing and repair: Fundamentals and applications, Addit. Manuf. 21 (2018) 628–650. https://doi.org/10.1016/j.addma.2018.04.017
[20] C. Chen, S. Gojon, Y. Xie, S. Yin, C. Verdy, Z. Ren, H. Liao, S. Deng, A novel spiral trajectory for damage component recovery with cold spray, Surf. Coat. Technol. 309 (2017) 719–728. https://doi.org/10.1016/j.surfcoat.2016.10.096
[21] P. Dupuis, Y. Cormier, M. Fenech, A. Corbeil, B. Jodoin, Flow structure identification and analysis in fin arrays produced by cold spray additive manufacturing, Int. J. Heat Mass Transf. 93 (2016) 301–313. https://doi.org/10.1016/j.ijheatmasstransfer.2015.10.019
[22] M.E. Lynch, W. Gu, T. El-Wardany, A. Hsu, D. Viens, A. Nardi, M. Klecka, Design and topology/shape structural optimisation for additively manufactured cold sprayed components: This paper presents an additive manufactured cold spray component which is shape optimised to achieve 60% reduction in stress and 20% reduction in weight, Virtual Phys. Prototyp. 8 (2013) 213–231. https://doi.org/10.1080/17452759.2013.837629
[23] Brothers In Arms: These Robots Put A New Twist On 3D Printing - GE Reports, (n.d.). https://www.ge.com/reports/brothers-arms-robots-put-new-twist-3d-printing/ (accessed September 24, 2019).
[24] About Titomic, (n.d.). https://www.titomic.com/how-it-began.html?searched=cold+spray&advsearch=oneword&highlight=ajaxSearch_highlight+ajaxSearch_highlight1+ajaxSearch_highlight2 (accessed September 27, 2019).
[25] C.J. Huang, H.J. Wu, Y.C. Xie, W.Y. Li, C. Verdy, M.-P. Planche, H.L. Liao, G. Montavon, Advanced brass-based composites via cold-spray additive-manufacturing and its potential in component repairing, Surf. Coat. Technol. 371 (2019) 211–223. https://doi:10.1016/j.surfcoat.2019.02.034.

[26] D. Kotoban, S. Grigoriev, A. Okunkova, A. Sova, Influence of a shape of single track on deposition efficiency of 316L stainless steel powder in cold spray, Surf. Coat. Technol. 309 (2017) 951–958. https://doi:10.1016/j.surfcoat.2016.10.052.
[27] Z. Cai, S. Deng, H. Liao, C. Zeng, G. Montavon, The effect of spray distance and scanning step on the coating thickness uniformity in cold spray process, J. Therm. Spray Technol. 23 (2014) 354–362. https://doi.org/10.1007/s11666-013-0002-0
[28] C. Chen, Y. Xie, C. Verdy, H. Liao, S. Deng, Modelling of coating thickness distribution and its application in offline programming software, Surf. Coat. Technol. 100 (2017) 315–325. https://doi.org/10.1016/j.surfcoat.2016.10.044
[29] C.J. Li, W.Y. Li, Y.Y. Wang, H. Fukanuma, Effect of spray angle on deposition characteristics in cold spraying, Therm. Spray. (2003) 91–96.
[30] H. Wu, X. Xie, M. Liu, C. Chen, H. Liao, Y. Zhang, S. Deng, A new approach to simulate coating thickness in cold spray, Surf. Coat. Technol. (2019) 125151. https://doi:10.1016/j.surfcoat.2019.125151.
[31] C.-J. Li, W.-Y. Li, H. Liao, Examination of the critical velocity for deposition of particles in cold spraying, J. Therm. Spray Technol. 15 (2006) 212–222. https://doi.org/10.1361/105996306X108093
[32] S. Yin, X. Wang, W. Li, B. Xu, Numerical study on the effect of substrate angle on particle impact velocity and normal velocity component in cold gas dynamic spraying based on CFD, J. Therm. Spray Technol. 19 (2010) 1155–1162. https://doi.org/10.1007/s11666-010-9510-3
[33] W.-Y. Li, S. Yin, X.-F. Wang, Numerical investigations of the effect of oblique impact on particle deformation in cold spraying by the SPH method, Appl. Surf. Sci. 256 (2010) 3725–3734. https://doi.org/10.1016/j.apsusc.2010.01.014
[34] K. Binder, J. Gottschalk, M. Kollenda, F. Gärtner, T. Klassen, Influence of impact angle and gas temperature on mechanical properties of titanium cold spray deposits, J. Therm. Spray Technol. 20 (2011) 234–242. https://doi.org/10.1007/s11666-010-9557-1